The spin-dependent transport of Co-encapsulated Si nanotubes contacted with Cu electrodes

Yan-Dong Guo,[1,2] Xiao-Hong Yan,[1,2,a)] and Yang Xiao[1]
[1]*College of Science, Nanjing University of Aeronautics and Astronautics, Nanjing 210016, China*
[2]*College of Electronic Science and Engineering, Nanjing University of Posts and Telecommunications, Nanjing 210046, China*

(Received 28 July 2013; accepted 31 January 2014; published online 11 February 2014)

Unlike carbon nanotubes, silicon ones are hard to form. However, they could be stabilized by metal-encapsulation. Using first-principles calculations, we investigate the spin-dependent electronic transport of Co-encapsulated Si nanotubes, which are contacted with Cu electrodes. For the finite tubes, as the tube-length increases, the transmission changes from spin-unpolarized to spin-polarized. Further analysis shows that, not only the screening of electrodes on Co's magnetism but also the spin-asymmetric Co-Co interactions are the physical mechanisms. As Cu and Si are the fundamental elements in semiconductor industry, our results may throw light on the development of silicon-based spintronic devices. © *2014 AIP Publishing LLC*.
[http://dx.doi.org/10.1063/1.4865589]

Spintronics is one of the most promising areas in nanoelectronics.[1–3] Nowadays, silicon is a fundamental element in semiconductor industry, so it is important to study its application in spintronics. So far, kinds of spin-related phenomena have been revealed in Si-based materials.[4–7] Unlike carbon nanotubes, silicon ones with hollow inside are hard to form, as sp^2 hybridization is not favorable in Si.[8,9] However, it is found that, Si cage clusters could be stabilized by metal encapsulation.[8,10,11] Moreover, they could be assembled together to form Si nanotubes.[12–14] In experiment, epitaxial self-assembled metal silicide nanowires (or nanotube bundles) have been synthesized,[15,16] and their stability as well as other properties have been studied by theoretical studies.[17] Previous studies show that $3d$ transition metal-doped Si nanotubes exhibit interesting magnetic properties,[13,18] which have great potential for fabricating Si-based spintronic devices. In the present work, we focus on the spin-dependent electronic transport of Co-doped Si nanotubes, which are contacted with Cu electrodes. For the finite tubes, as the tube-length increases, the transmission changes from spin-unpolarized to spin-polarized. It is found that, the transition is induced not only by the screening of electrodes on the magnetic moment of Co, but also by the spin-asymmetric Co-Co interactions. As both Cu and Si are the fundamental elements in semiconductor industry, we believe our results are useful for the designing of Si-based spintronic devices.

To explore the transport properties of the system accurately, density functional theory (DFT) calculations combined with nonequilibrium Green's function (NEGF) are performed, which are carried out through the Atomistix Toolkit package.[19,20] We use the mesh cutoff energy of 150 Ry, and $4 \times 4 \times 50$ k-point mesh in the Monkhorst-Park scheme.[21] As the system contains transition metal atoms, Perdew-Burke-Eenzerhof (PBE) formulation of the generalized gradient approximation (GGA) is used as the exchange-correlation function.[22] Double-zeta basis set is chosen to be the local numerical orbitals, with which the transmission spectra are in good agreement with former results.[23] The nanotubes are fully optimized until all the forces are less than 0.05 eV/Å. By minimizing the total energy of the whole system, the distance between electrodes and Si nanotube is optimized to be 2.35 Å.

In NEGF theory, the current is obtained according to the Landauer-Büttiker formula

$$I(V)_{\uparrow\downarrow} = \frac{2e}{h}\int T(E,V)_{\uparrow\downarrow}[f(E-\mu_L) - f(E-\mu_R)]dE,$$

where $\mu_{L/R}$ is the chemical potential of the left or right electrode, $f(E-\mu_{L/R})$ is the Fermi function in the left or right electrode, and $V = (\mu_L - \mu_R)/e$ defines the bias window. $T(E,V)_{\uparrow\downarrow}$ is the transmission probability through the system for up- or down-spin, which is calculated from (the denotation of spin is omitted)

$$T(E,V) = Tr[\Gamma_L(E,V)G^R(E,V)\Gamma_R(E,V)G^A(E,V)],$$

where $G^{R/A}(E,V)$ is the retarded or advanced Green's function of the scattering region, and $\Gamma_{L/R}$ is the coupling matrix to the left or right electrode. In this paper, we focus on the zero-bias ($V = 0$) condition, as the transport under low bias is largely dominated by it.

For clarity, the Co-doped Si nanotubes are denoted as $Si_{6N+6}Co_N$, where N = 1, 2, 3, and 4. The right panel of Fig. 1(b) presents the cross-section of the tubes. Most commonly used materials of electrodes are Cu, Al, Au, and Ag, and they all possess face centered cubic (fcc) structure. Like the cross-section of the Si tube, fcc(111) surface exhibits hexagonal lattice geometry, as shown in Fig. 1(b). Among these four metals, the structural parameter of Cu(111) matches the best with that of Si nanotube [see Fig. 1(b) for details]. Besides, it is a fundamental element in integrated circuit (IC), so Cu is chosen to be the electrode material, with the (111) surface to be the contact surface.

a)Electronic mail: xhyan@nuaa.edu.cn

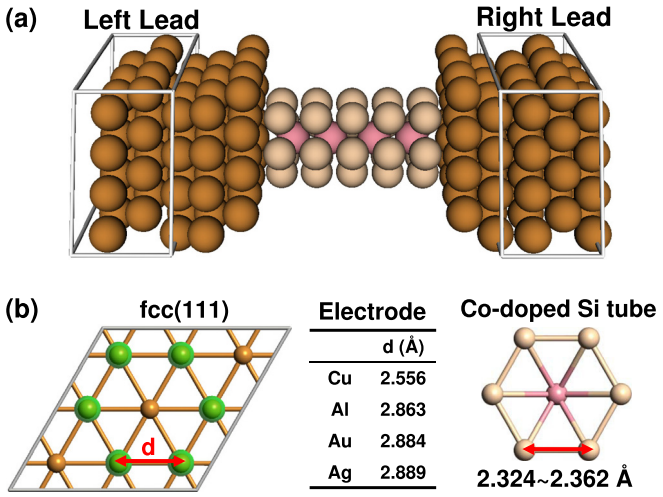

FIG. 1. (a) Geometric view of the Cu-$Si_{6N+6}Co_N$-Cu system (here, N = 4), and (b) the structural parameters for bulk metals (Cu, Al, Au, and Ag) and Si nanotubes. The supercell of electrodes in (a) is larger than that of (b) (left panel) to eliminate the interactions between Si nanotube and its adjacent images.

The setup of the whole two-probe system (Cu-$Si_{6N+6}Co_N$-Cu) is shown in Fig. 1(a) (take N = 4 as an example). The solid and white boxes indicate the supercells of the electrodes. Due to the periodicity and the size of supercells, the interactions between neighboring nanotubes exist. But they have no material impact on the transmission and magnetic properties, and this has been checked by comparing our results with previous studies.[13,23]

We calculate the spin-dependent transmission spectra for each configuration, Cu-$Si_{6N+6}Co_N$-Cu (N = 1, 2, 3, and 4), shown in Fig. 2. One finds the transmission of N = 1 tube [Fig. 2(a)] is spin-unpolarized, in accordance with former results.[23] However, when the tube becomes longer (N = 2–4), all the spectra become spin-polarized [Figs. 2(b)–2(d)]. From structural point of view, longer tubes are composed of short ones, so the transition of the transmission is interesting. In the following, we will find out the underlying physical mechanisms of this phenomenon.

To observe the magnetic properties, we performed the calculation of mulliken population. Table I shows the

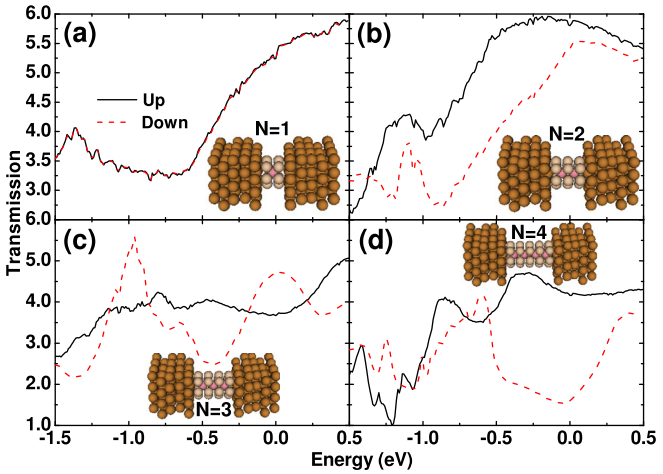

FIG. 2. Spin-dependent transmission spectra of Cu-$Si_{6N+6}Co_N$-Cu system. (a)–(d) N = 1–4. Up-spin: solid and black line, and down-spin: dashed and red line. Zero energy is set to be the Fermi level.

TABLE I. The average mulliken population per Co atom in Cu-$Si_{6N+6}Co_N$-Cu (N = 1, 2, 3, and 4) for up-spin, down-spin, and their difference (i.e., the magnetic moment). N is the number of Co atoms in the tube. 2(3) and 1(3) correspond to the configurations in Figs. 3(c) and 3(d), respectively.

N	Up	Down	Up-down (μ_B)
1	4.153	4.142	0.011
2	4.716	3.699	1.017
3	4.580	3.867	0.713
4	4.697	3.777	0.920
2(3)	4.262	4.086	0.176
1(3)	4.576	3.757	0.819

average mulliken population per Co atom in each nanotube for up-spin, down-spin, and their difference (up-down, i.e., the magnetic moment), respectively. In N = 1 case, the magnetic moment of Co is only 0.011 μ_B. In former studies, Kong and Chelikowsky[23] proposed that electrodes would screen the magnetic moment of Co. In our system, the two sides of the Co atom in $Si_{12}Co_1$ are both contacted by Cu electrodes, so the screening of the electrodes makes the magnetic moment of Co decrease to almost zero. As a result, the transmission of N = 1 case is spin-unpolarized.[23] Obviously, when the tube becomes longer, the screening effect on the inner Co atoms will be weakened, where the magnetic moment should be larger. As one finds in Table I, the magnetic moments (up-down) of N = 2–4 cases are indeed much larger than that of N = 1. So, the spin-polarization of the transmission is induced by these magnetic moments. However, the large polarization $[(T_\uparrow - T_\downarrow)/(T_\uparrow + T_\downarrow)]$, especially at the Fermi level (0 eV) of N = 4 case, suggests that there might be some other mechanisms for the large spin-polarization. Next, we demonstrate that the Co-Co interaction also plays an important role.

In N = 4 case, the magnetic moment is not the largest (Table I). However, at the Fermi level, as shown in Fig. 2(d), its spin-polarization of the transmission is the largest. In order to find out another source of spin-polarization, we remove all the Co atoms in $Si_{18}Co_2$ and $Si_{24}Co_3$ (this removing method is only for analysis purpose, and the geometric structures left are not optimized, which actually are unstable). After removing, the spin-dependent transport spectra are shown in Figs. 3(a) and 3(b). Both of them become spin-unpolarized, so the spin-polarization is no doubt induced by the doped metal (Co), rather than Si or Cu.

If we only remove the middle Co atom in $Si_{24}Co_3$, then we get $Si_{24}Co_2$ [Fig. 3(c)]. For $Si_{24}Co_2$, the transmission exhibits slightly spin-polarized. As mentioned before, electrodes could screen the magnetic moment of Co. However, compared with the transmission of $Si_{18}Co_2$ in Fig. 2(b), the spin-polarization of $Si_{24}Co_2$ is much smaller than that. These two configurations [Figs. 3(c) and 2(b)] both own two Co atoms, which are all adjacent to the electrodes. So, the screening effect should be the same. However, their transmission spectra exhibit a big difference. It should be noted that the Co-Co distances in the two cases are different. Large distance [$Si_{24}Co_2$, Fig. 3(c)] induces small spin-polarization, and small distance [$Si_{18}Co_2$, Fig. 2(d)] induces large spin-polarization. This indicates that the Co-Co interaction

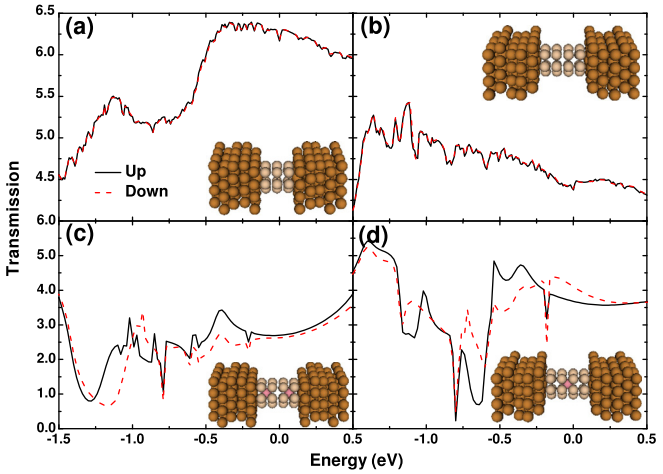

FIG. 3. Spin-dependent transmission spectra of Cu-nanotube-Cu for (a) Si_{18}, (b) Si_{24}, (c) $Si_{24}Co_2$, and (d) $Si_{24}Co$. The structures in (a) and (b) are obtained by removing the Co atoms in $Si_{18}Co_2$ and $Si_{24}Co_3$, respectively. (c) $Si_{24}Co_2$ is obtained by removing the middle Co atom in $Si_{24}Co_3$, and (d) $Si_{24}Co$ is obtained by removing the other two Co atoms in $Si_{24}Co_3$. Zero energy is set to be the Fermi level.

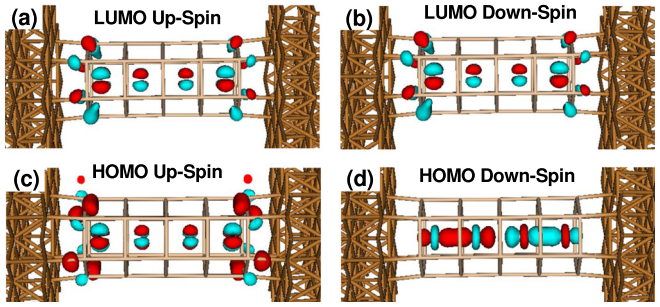

FIG. 4. The spatial distributions of LUMO and HOMO states for the $Si_{30}Co_4$ nanotube, after the process of molecular projected self-consistent Hamiltonian. (a) and (b) for up- and down-spins of LUMO, respectively. (c) and (d) for up- and down-spins of HOMO, respectively.

also plays an important role. To confirm that, we construct another configuration, $Si_{24}Co$ [Fig. 3(d)], by removing the two Co atoms located at the two sides of $Si_{24}Co_3$ [Fig. 2(c)]. Away from the electrodes, the Co atom inside could be seen as not being screened. Now the Co atom only induces slight spin-polarization [Fig. 3(d)], although larger magnetic moment presents [0.819 μ_B, see Table I, N = 1(3)]. Through a rough estimation, we simply add the spin-polarizations of $Si_{24}Co_2$ [Fig. 3(c)] and $Si_{24}Co$ [Fig. 3(d)] and compare the sum with that of $Si_{24}Co_3$ [Fig. 2(c)]. In structure, the two side Co and one middle Co atoms construct all the Co atoms in $Si_{24}Co_3$ [Fig. 2(c)]. As discussed before, the Si atoms do not contribute to the spin-polarization. Thus, we could add and roughly compare their spin-polarizations. Apparently, the sum of the polarizations [Figs. 3(c) and 3(d)] is still not as large as the polarization in $Si_{24}Co_3$ [Fig. 2(c)]. It is because the interaction between adjacent Co atoms is ignored in the "simple-adding" procedure.

Among the four cases in Fig. 2, the spectra of $Si_{30}Co_4$ [Fig. 2(d)] at the Fermi level (0 eV) exhibit the largest spin-polarization. If the Co-Co interaction really plays an important role in the transport, it should behave obviously near the Fermi level in $Si_{30}Co_4$ [Fig. 2(d)]. We here calculate the molecular projected self-consistent Hamiltonian (MPSH) for $Si_{30}Co_4$ and plot the highest occupied molecular orbital (HOMO) and lowest unoccupied molecular orbital (LUMO) for both spins in Fig. 4. The MPSH is defined to be the Hamiltonian of a transport system projected onto a subset of atoms, which usually locate in the scattering region (e.g., the Co-doped Si nanotube in the two-probe system). After the projection of Hamiltonian, the subset of atoms would be treated as an isolated molecule. Its energy spectrum, as well as the HOMO and LUMO states, is given out by diagonalizing the new Hamiltonian. Different from the real isolated molecule, the influence of the electrodes has been included in the molecular states. In other words, MPSH could help us to observe the molecular orbitals after taking into account the effect of electrodes.

In Fig. 2, the bonds are omitted, and each atom is represented by a ball (including Cu, Co, and Si). In Fig. 4, in order to see the HOMO (or LUMO) states more clearly, the balls representing the atoms are not shown, and only some bonds (sticks) are plotted. One finds that around Co atoms, the LUMO states are in the shape of four pear-shaped lobes, belonging to the *d*-orbitals of Co. There are also some distributions at the interfaces between Si-tube and electrodes. Most importantly, the distributions of LUMO states are almost the same for up- and down-spins [Figs. 4(a) and 4(b)].

However, for HOMO sates, the distributions are quite different between up- and down-spins [Figs. 4(c) and 4(d)]. For up-spin, the distribution of HOMO [Fig. 4(c)] is the same as that of LUMO [Figs. 4(a) and 4(b)]. While for down-spin [Fig. 4(d)] around Co atoms, the distributions of HOMO are no longer in the shape of four pear-shaped lobes. Each of them exhibits the dumbbell shape of d_{z^2}-orbital. The left two (or right two) d_{z^2}-orbitals overlap with each other to form an anti-δ bond. This is consistent with the analysis of geometric structure. For facility, we denote the four Co atoms with Co_1, Co_2, Co_3, and Co_4 from left to right. The corresponding distances between adjacent Co atoms are 2.60, 3.02, and 2.59 Å, respectively. One finds the distances of Co_1-Co_2 (2.60 Å) and Co_3-Co_4 (2.59 Å) are almost the same. They are both smaller than that of Co_2-Co_3 (3.02 Å). This difference indicates the forming of the two anti-δ bonds, which are contributed by the down-spin states. Thus, the Co-Co interaction is spin-asymmetric and that results in the large spin-polarization of the transmission. Thus, not only the influence of electrodes, but also the Co-Co interactions play an important role in the spin-dependent transport of the system.

In this paper, we focus on the finite tubes. Former studies show that the infinite Co-doped Si nanotube is nonmagnetic,[13] different from finite ones. This is due to the different positions of Co atoms in the finite and infinite Si nanotubes. In the former case, each Co atom is placed between Si_6 layers (see the insets of Fig. 2), whereas in the latter case, the Co atoms are located in the Si_6 layers.[13] Apparently, in the finite tube, the Si-Co bond lengths are larger than those in the infinite ones. It has been found that strong hybridization between *sp* states of Si and *d* states of metal would quench the magnetic moments of the dopants.[13] Thus, the infinite Co-doped Si nanotube shows nonmagnetic. Similarly, the *s* orbitals of Cu electrodes have the same effect as the *sp*

orbitals of Si in quenching the magnetic moment. So, the magnetic moment of Co at the end of the tube would be screened by the electrodes. On the contrary, in the Co-Co interaction, the hybridization of *d-d* orbitals usually enhances the magnetic moments, as we have discussed above.

In summary, we studied the spin-dependent electronic transport of Co-encapsulated Si nanotubes contacted with Cu electrodes through first-principle calculations. For the finite nanotubes, as the tube-length increases, the transmission changes from spin-unpolarized to spin-polarized. Further analysis shows that not only the screening effect of Cu electrodes, but also the spin-asymmetric Co-Co interactions in the nanotube are the underlying physical mechanisms. As Cu and Si are fundamental elements in the semiconductor industry, we believe our results will be useful for the development of silicon-based spintronic devices.

This work was supported by the National Natural Science Foundation of China (NSFC51032002 and NSFC11247033), the Key Project of National High Technology Research and Development Program of China (2011AA050526), and the Fundamental Research Funds for the Central Universities (NS2014073).

[1]A. Fert, Rev. Mod. Phys. **80**, 1517 (2008).
[2]I. Žutić, J. Fabian, and S. Sarma, Rev. Mod. Phys. **76**, 323 (2004).
[3]D. Awschalom and M. Flatté, Nat. Phys. **3**, 153 (2007).
[4]R. Jansen, Nature Mater. **11**, 400 (2012).
[5]M. Flatté, Nature **462**, 419 (2009).
[6]I. Žutić and J. Fabian, Nature **447**, 268 (2007).
[7]I. Appelbaum, B. Huang, and D. J. Monsma, Nature **447**, 295 (2007).
[8]H. Hiura, T. Miyazaki, and T. Kanayama, Phys. Rev. Lett. **86**, 1733 (2001).
[9]M. Broyer, M. Pellarin, B. Baguenard, J. Lerme, J. L. Vialle, P. Melinon, J. Tuaillon, V. Dupuis, B. Prevel, and A. Perez, *Cluster Assembled Materials*, edited by K. Sattler, Vol. Material Science Forum 232 (Trans Tech Publications, Zurich-Utikon, 1996), p. 27.
[10]S. M. Beck, J. Chem. Phys. **87**, 4233 (1987).
[11]V. Kumar and Y. Kawazoe, Phys. Rev. Lett. **87**, 45503 (2001).
[12]A. K. Singh, V. Kumar, T. M. Briere, and Y. Kawazoe, Nano Lett. **2**, 1243 (2002).
[13]A. Singh, T. Briere, V. Kumar, and Y. Kawazoe, Phys. Rev. Lett. **91**, 146802 (2003).
[14]T. Dumitrică, M. Hua, and B. Yakobson, Phys. Rev. B **70**, 241303 (2004).
[15]Y. Chen, D. A. A. Ohlberg, and R. S. Williams, J. Appl. Phys. **91**, 3213 (2002).
[16]Y. Chen, D. A. A. Ohlberg, G. Medeiros-Ribeiro, Y. A. Chang, and R. S. Williams, Appl. Phys. Lett. **76**, 4004 (2000).
[17]N. G. Szwacki and B. I. Yakobson, Phys. Rev. B **75**, 035406 (2007).
[18]Y. R. Jang, C. Jo, and J. I. Lee, IEEE Trans. Magn. **41**, 3118 (2005).
[19]M. Brandbyge, J.-L. Mozos, P. Ordejón, J. Taylor, and K. Stokbro, Phys. Rev. B **65**, 165401 (2002).
[20]J. Taylor, H. Guo, and J. Wang, Phys. Rev. B **63**, 245407 (2001).
[21]H. J. Monkhorst and J. D. Pack, Phys. Rev. B **13**, 5188 (1976).
[22]J. P. Perdew, K. Burke, and M. Ernzerhof, Phys. Rev. Lett. **77**, 3865 (1996).
[23]L. Kong and J. Chelikowsky, Phys. Rev. B **77**, 073401 (2008).